Journal of Inflammation Research

Dovepress
Taylor & Francis Group

Open Access Full Text Article

ORIGINAL RESEARCH

Lysophosphatidylcholine as a Novel Diagnostic Biomarker in Kawasaki Disease: Based on Immunometabolism-Related Signature

Xiaomei Ma[1,*], Yang Zheng[2,*], Chenhui Feng[1], Mingming Zhang[3], Hongmao Wang[3], Xiaohui Li[1–3]

[1]Capital Institute of Pediatrics-Peking University Teaching Hospital, Beijing, People's Republic of China; [2]Capital Institute of Pediatrics, Chinese Academy of Medical Sciences, Peking Union Medical College, Beijing, People's Republic of China; [3]Department of Cardiovascular Medicine, Capital Center for Children' s Health, Capital Medical University, Beijing, People's Republic of China

*These authors contributed equally to this work

Correspondence: Xiaohui Li, Capital Institute of Pediatrics-Peking University Teaching Hospital, No. 2, Yabao Road, Chaoyang District, Beijing, 100020, People's Republic of China, Email lxhmaggie@pumc.edu.cn

Purpose: Kawasaki disease (KD) is a systemic vasculitis of unknown etiology. Delayed diagnosis and treatment elevate the risk of coronary artery complications. This study aims to investigate metabolic disorders associated with its potential pathophysiology and to explore novel diagnostic biomarkers.

Patients and Methods: Untargeted metabolomics was used to identify significantly dysregulated metabolic pathways in patients with KD. Targeted lipidomic analysis was performed to detect differentially expressed lipid metabolites. Candidate plasma biomarkers were quantified using ELISA. Single-cell RNA sequencing was used to analyze the expression of lipid metabolism-related genes and cellular heterogeneity.

Results: Sphingolipid metabolism was confirmed to be dysregulated in patients with KD. Twelve differentially expressed lipid species were identified: 20:5-carnitine, sphingomyelin 32:2;O2, ceramide d16:0/24:0, glucosylceramide d18:1/26:0, lysophosphatidylcholine (LPC) O-16:0, LPC 17:0, LPC 18:0, and phosphatidylcholine (PC) 32:2, PC 36:3, PC 40:3, PC 40:4, and PC 40:7. ELISA validation confirmed the lipidomics-identified alterations in LPC. As a diagnostic biomarker, LPC achieved an area under the curve (AUC) of 0.768, with 64.7% sensitivity and 88.2% specificity. Single-cell RNA sequencing data revealed a marked accumulation of monocytes in KD, along with upregulated expression of lipid metabolism-associated genes. Notably, the expression levels of inflammatory genes were altered along with those of LPC degradation-related genes in monocytes from patients with KD.

Conclusion: This study demonstrated significant dysregulation of lipid metabolism in KD, potentially driven by inflammatory responses in monocytes. LPC has emerged as a potential biomarker of KD and provides new insights into its early diagnosis.

Keywords: Kawasaki disease, metabolomics, targeted lipidomics, single-cell RNA sequencing, lysophosphatidylcholine

Introduction

Kawasaki disease (KD) is an acute febrile illness characterized by immune-mediated systemic vasculitis that primarily affects children under 5 years of age.[1] This disease has substantial public health implications because its hallmark complication, coronary artery lesions (CAL), is a leading cause of acquired heart disease in children across developed nations.[1] Timely diagnosis and clinical intervention have reduced the incidence of coronary artery aneurysms from 25% to 4%.[2] Nevertheless, the diagnosis of KD still relies on the assessment of clinical symptoms along with nonspecific laboratory tests, which remains a challenge for frontline pediatricians. Conventional serological indicators,[3–5] including C-reactive protein (CRP), platelet count, erythrocyte sedimentation rate (ESR), and albumin, have demonstrated limited discriminatory power for KD. Additional biomarkers, including ferritin, tumor necrosis factor-alpha (TNF-α), and interleukin (IL)-6, exhibit overlapping changes in pathogenic infections and other autoimmune disorders.[6–8]

Received: 22 October 2025
Accepted: 19 December 2025
Published: 31 December 2025

Consequently, there is a clinical need to develop specific diagnostic markers for the early diagnosis of KD. Advances in multi-omics technology have enabled the exploration of novel candidate biomarkers.

Metabolomics provides a highly sensitive and comprehensive analysis of physiological and pathological metabolic dysregulation during disease progression.[9,10] Recent studies have highlighted the multidimensional clinical associations between metabolic dysregulation and KD, including dynamic evolution across treatment phases,[11] variations in treatment responsiveness,[12] and specific metabolic signatures associated with the severity of CAL.[13,14] Despite growing evidence linking metabolic dysregulation to KD clinical features, lipid metabolism persists as a key yet under-investigated component, with its specific role and diagnostic biomarker potential awaiting exploration.

Single-cell RNA sequencing (scRNA-seq) has transformed our understanding of KD by revealing previously unrecognized immune cell heterogeneity. Our previous studies have built upon this foundation, systematically delineating the immune landscape of KD and identifying a vigorous inflammatory storm in cases complicated with CAL.[15] Critically, such immune dysregulation is increasingly recognized to be intertwined with profound metabolic reprogramming.[16] However, a systematic investigation integrating these two critical aspects is still lacking in KD research.

Therefore, this study applied metabolomics to characterize the metabolic profile of KD and integrated single-cell transcriptome data to investigate the relationship between metabolic aberration and immune-inflammatory activation, thereby offering novel metabolic insights and potential translational opportunities for the early diagnosis of KD.

Materials and Methods

Study Design and Participants

Between January 2022 and December 2024, 196 participants were recruited from the Capital Center for Children's Health, Capital Medical University, comprising 75 patients with KD, 50 febrile controls (FC), and 71 healthy controls (HC). Among these participants, 181 were included in the biomarker discovery and validation sets, and 15 underwent scRNA-seq analysis. Complete KD was diagnosed based on the American Heart Association guidelines.[2] Patients in the FC group were diagnosed with infectious fever at our center during the study period. The HC group consisted of children who displayed no symptoms of infection during the previous 2 weeks. Participants with any of the following conditions were excluded from the study: recurrent KD, obesity, malignant tumors, endocrine diseases, systemic inflammatory disorders, autoimmune diseases, or a positive SARS-CoV-2 test. All controls were age- and sex-matched to patients with KD.

Demographic and laboratory parameters were collected from all participants, including age, sex, body mass index (BMI), white blood cell count (WBC), neutrophil percentage (N%), CRP, procalcitonin (PCT), ESR, and cytokines (TNF-α, IL-6, IL-2 receptor, and IL-1). Maximal coronary artery diameters, obtained from echocardiography, were converted to Z-scores (Z-max) based on the Kabayashi formula,[17] and a Z-score > 2 was designated as CAL.[1,2] Peripheral blood was collected following a confirmed diagnosis and prior to intravenous immunoglobulin (IVIG) treatment. This study was approved by the Ethics Committee of the Capital Institute of Pediatrics and complied with the Declaration of Helsinki.

Plasma Metabolomics Analysis

All serum samples from the discovery set were subjected to liquid chromatography-tandem mass spectrometry (LC-MS/MS) analyses. We conducted an untargeted metabolomic analysis on Dataset 1, which consisted of patients with KD (n = 20) and HC (n = 20), to identify key metabolic dysregulations in KD. Untargeted metabolomics was performed on a Triple Quad 5600+ system via normal-phase chromatography (1 μL injection; mobile phase: 50% acetonitrile/10 mM ammonium acetate, pH 9) with negative ion mode MS/MS acquisition (m/z 80–1200; resolution 70,000 full-scan/17,500 MS/MS). Progenesis QI was used to process the data for feature extraction, peak alignment, SVR normalization, and QC filtration (>50% missing value exclusion). Metabolite identification integrated in-house and public databases.

Further targeted lipidomics was implemented in Dataset 2, which included 30 patients with KD, 30 FC, and 30 HC. Lipidomic analysis was performed using ExionLC-AD–Sciex QTRAP 6500 PLUS. Polar lipids were separated by NP-HPLC on a TUP-HB silica column (150 × 2.1 mm, 3 μm) with mobile phase A (chloroform: methanol: ammonium

hydroxide, 89.5:10:0.5) and B (chloroform: methanol: ammonium hydroxide: water, 55:39:0.5:5.5). MRM transitions enabled polar lipid comparisons. The internal standards used were d_9-phosphatidylcholine (PC) 32:0, d_9-PC36:1p, d_3-16:0 carnitine, ceramide (Cer) (d18:1/15:0-d_7), d_9-sphingomyelin (SM), C8-Glu/galactosylceramide, d_3-lactosylceramides, globotriaosylceramide, d_7-lysophosphatidylcholine (LPC) 18:1, and d_{17}:1 sphingosine/sphingosine-1-phosphate (Avanti Polar Lipids).

ELISA Analysis of Key Lipid Species

Serum samples from the validation set, including 17 patients with KD, 17 FC, and 17 HC, were assayed for LPC and Cer levels following the kit instructions. Technical replicates were performed in triplicate to ensure data precision.

ScRNA-Seq and Data Analysis

To further delineate lipid metabolism-related gene expression across immune cell subtypes, single-cell data were analyzed from 15 participants, comprising 8 patients with KD, 3 FC, and 4 HC. Peripheral blood mononuclear cells (PBMCs) were isolated from whole blood by centrifugation using red blood cell lysis buffer (Miltenyi Biotec). Single-cell 5' libraries were prepared with the 10X Genomics Chromium Controller Instrument. After quality control assessment, the libraries were sequenced on an Illumina platform (Illumina, San Diego, CA, USA). Raw and filtered gene expression matrices were processed using the kallisto/bustool (v0.24.4) pipeline and subjected to rigorous quality control. Subsequently, normalization and natural logarithm transformation were performed to prepare the data for downstream analysis. Highly variable genes were selected, followed by principal component analysis-based dimensionality reduction and batch effect correction using a harmony algorithm to integrate single-cell data across different batches. Unsupervised cell clustering was performed using the Louvain algorithm (the sc.tl.louvain function in ScanPy). Cell state scores were calculated using the sc tl.score_gene function of ScanPy.

Statistical Analysis

Statistical analyses were performed using R version 4.3.1. Continuous data are presented as mean ± standard deviation or median (interquartile range (IQR)) for normally distributed or non-normally distributed variables, respectively. Group comparisons were performed using the Student's *t* test for normally distributed data and the Mann–Whitney *U*-test for non-normally distributed data. For multi-group comparisons, the Kruskal–Wallis test was applied, followed by Dunn's post hoc test for pairwise comparisons if a significant difference was detected. The mean importance measure of the random forest algorithm was used for metabolite selection. Receiver operating characteristic curves (ROC) were used to evaluate the diagnostic performance of the biomarkers. Correlations between differentially expressed lipids and clinical parameters were analyzed using Spearman' s correlation. Differences were considered statistically significant at $P < 0.05$.

Results

General Information for Participants

The discovery and validation sets comprised 181 participants, with a median age of 34 months (14–53), including 98 (54%) boys and 83 (46%) girls. Among them were 67 patients with KD, who had a median age of 36 months (16–56.5) and consisted of 37 (55%) boys and 30 (45%) girls. Additionally, there were no significant differences in the levels of BMI, WBC, N%, CRP, PCT, ESR, cytokines, and Z-max across the KD groups in Dataset 1, Dataset 2, and the validation set, suggesting consistent baseline characteristics (all $P > 0.05$) (Table 1). 15 participants were included in the scRNA-seq analysis; their demographic characteristics are presented in Table S1.

Lipid Metabolism Was Altered in Patients with KD

As illustrated in Figure 1A and E, patients with KD were clearly distinguished from HC based on their metabolic profiles (orthogonal partial least squares discriminant analysis (OPLS-DA): $R^2Y = 0.995$, $Q^2 = 0.93$). By applying stringent screening criteria (Variable importance in the projection (VIP) > 1, FC > 2/< 0.5, and $P < 0.05$), 892 HMDB-annotated metabolites were identified, including 430 upregulated and 462 downregulated species in the KD group. In the Kyoto

Table 1 Participant Demographics and Laboratory Characteristics

	Discovery Set					Validation Set		
	Dataset 1		Dataset 2					
Variables	**KD (n=20)**	**HC (n=20)**	**KD (n=30)**	**FC (n=30)**	**HC (n=30)**	**KD (n=17)**	**FC (n=17)**	**HC (n=17)**
Age (m)	23.50 (13.75, 43.25)	21.50 (16.25, 37.25)	39.50 (16.75, 58.00)	31.00 (13.25, 55.00)	33.00 (13.25, 48.00)	48.00 (16.00, 60.00)	46.00 (16.00, 57.00)	44.00 (17.00, 49.00)
M/F	13/7	13/7	15/15	15/15	15/15	9/8	9/8	9/8
BMI (kg/m^2)	16.00 (15.12, 17.43)	NA	15.39 (14.49, 16.87)	14.83 (14.09, 16.06)	NA	15.34 (14.06, 16.53)	14.25 (11.50, 28.00)	NA
WBC ($10^9/L$)	14.09±5.64	NA	13.54±4.63	10.66±4.39	NA	13.16±5.80	10.23±4.81	NA
N (%)	65.15 (54.35, 73.97)	NA	66.25 (60.00, 72.20)	41.60 (32.83, 60.17)	NA	71.50 (58.50, 78.30)	48.00 (32.70, 59.20)	NA
CRP (mg/L)	57.49 (29.77, 86.28)	NA	63.29 (31.08, 83.89)	2.50 (0.80, 3.68)	NA	46.37 (26.32, 109.59)	2.60 (0.80, 3.60)	NA
PCT (ng/mL)	1.24 (0.14, 1.76)	NA	0.96 (0.12, 0.87)	0.10 (0.05, 0.25)	NA	0.43 (0.19, 1.00)	0.07 (0.05, 0.14)	NA
ESR (mm/h)	70.00 (47.50, 81.50)	NA	75.50 (61.75, 85.00)	NA	NA	75.00 (46.00, 85.00)	NA	NA
TNF-α (pg/mL)	16.35 (13.93, 23.02)	NA	21.10 (13.38, 25.98)	NA	NA	23.70 (20.00, 30.30)	NA	NA
IL-6 (pg/mL)	24.25 (10.29, 49.25)	NA	20.85 (7.70, 29.88)	NA	NA	35.90 (12.00, 53.00)	NA	NA
IL-2R (U/mL)	1826.00 (912.20, 2287.20)	NA	1514.00 (923.00, 2285.00)	NA	NA	1495.00 (1180.00, 2286.00)	NA	NA
IL-1 (pg/mL)	8.42 (5.00, 10.45)	NA	10.75 (5.24, 20.55)	NA	NA	5.7(5.00, 15.50)	NA	NA
Z-max	1.76 (1.14, 2.16)	NA	1.15 (0.79, 1.66)	NA	NA	1.17 (0.74, 1.55)	NA	NA

Abbreviations: KD, Kawasaki disease; FC, febrile control; HC, healthy control; BMI, body mass index; M, male; F, female; N(%), neutrophil percentage; Z-max, maximal coronary artery Z- score measured before IVIG treatment; NA, not applicable.

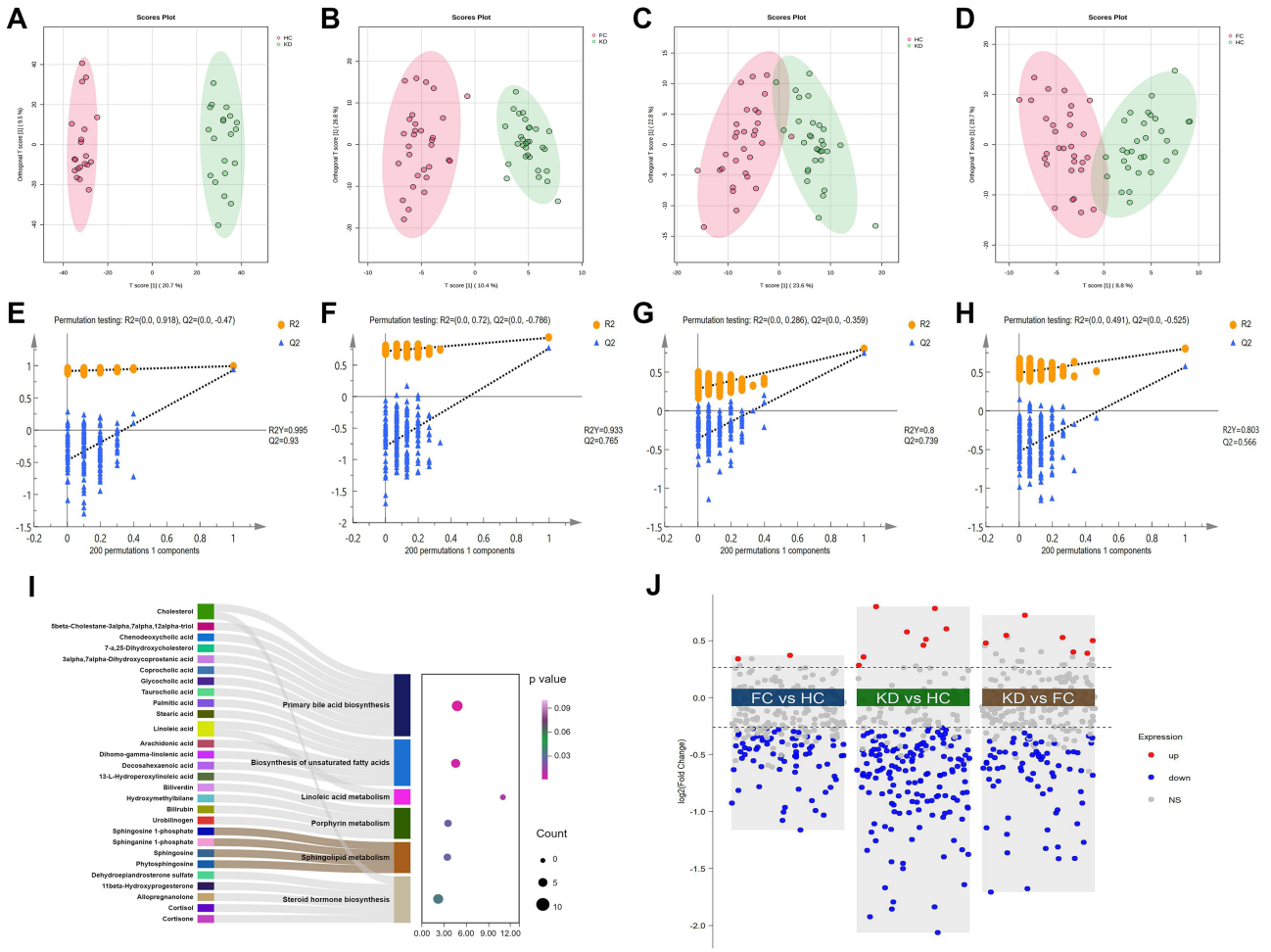

Figure 1 Peripheral blood metabolomic landscape of patients with KD. (**A**) The OPLS-DA model for the KD and HC groups based on untargeted metabolomics. (**B–D**) OPLS-DA models generated using targeted lipidomics for pairwise comparisons: KD vs FC, KD vs HC, and FC vs HC. (**E–H**) Statistical validation of the corresponding model using permutation analysis (200 iterations). (**I**) Sankey diagram showing altered metabolic pathways. The x-axis represents the rich factor, and the bubble size represents the number of differential metabolites annotated to this pathway. The y-axis represents the P-value, with smaller values positioned higher along the axis. Brown indicates the sphingolipid metabolic pathway. (**J**) Multiple volcano plots showing the comparison of differential lipid species between different groups (KD vs FC, KD vs HC, and FC vs HC).

Encyclopedia of Genes and Genomes (KEGG) pathway enrichment analysis, six significantly altered pathways were mapped: primary bile acid biosynthesis, unsaturated fatty acid biosynthesis, linoleic acid metabolism, porphyrin metabolism, sphingolipid metabolism, and steroid hormone biosynthesis (Figure 1I).

To prioritize sphingolipid metabolism among the six significantly disturbed pathways, we implemented targeted lipidomics in independent Dataset 2. After quality control, hundreds of lipid species spanning 13 lipid classes — carnitines, sphingosine, SM, Cer, globotriaosylceramide, ceramide-1-phosphate, sphingosine-1-phosphate, lactosylceramides, glucosylceramide (GluCer), galactosylceramide, PC, ether PC, and LPC — were detected via LC-MS/MS. The OPLS-DA model, coupled with external permutation tests, was employed to perform pairwise comparisons among the three predefined groups: KD vs FC ($R^2Y = 0.933$, $Q^2 = 0.765$) (Figure 1B and F), KD vs HC ($R^2Y = 0.8$, $Q^2 = 0.739$) (Figure 1C and G), and FC vs HC ($R^2Y = 0.803$, $Q^2 = 0.566$) (Figure 1D and H), revealing distinct intergroup separations and confirming the robustness and reliability of the model. According to the screening criteria (VIP > 1, FC > 1.2/< 0.83, and $P < 0.05$), we identified differential lipid species, yielding 77, 113, and 71 hits in the KD vs FC, KD vs HC, and FC vs HC comparisons, respectively, and visualized them using volcano plots (Figure 1J).

https://doi.org/10.2147/JIR.S567612

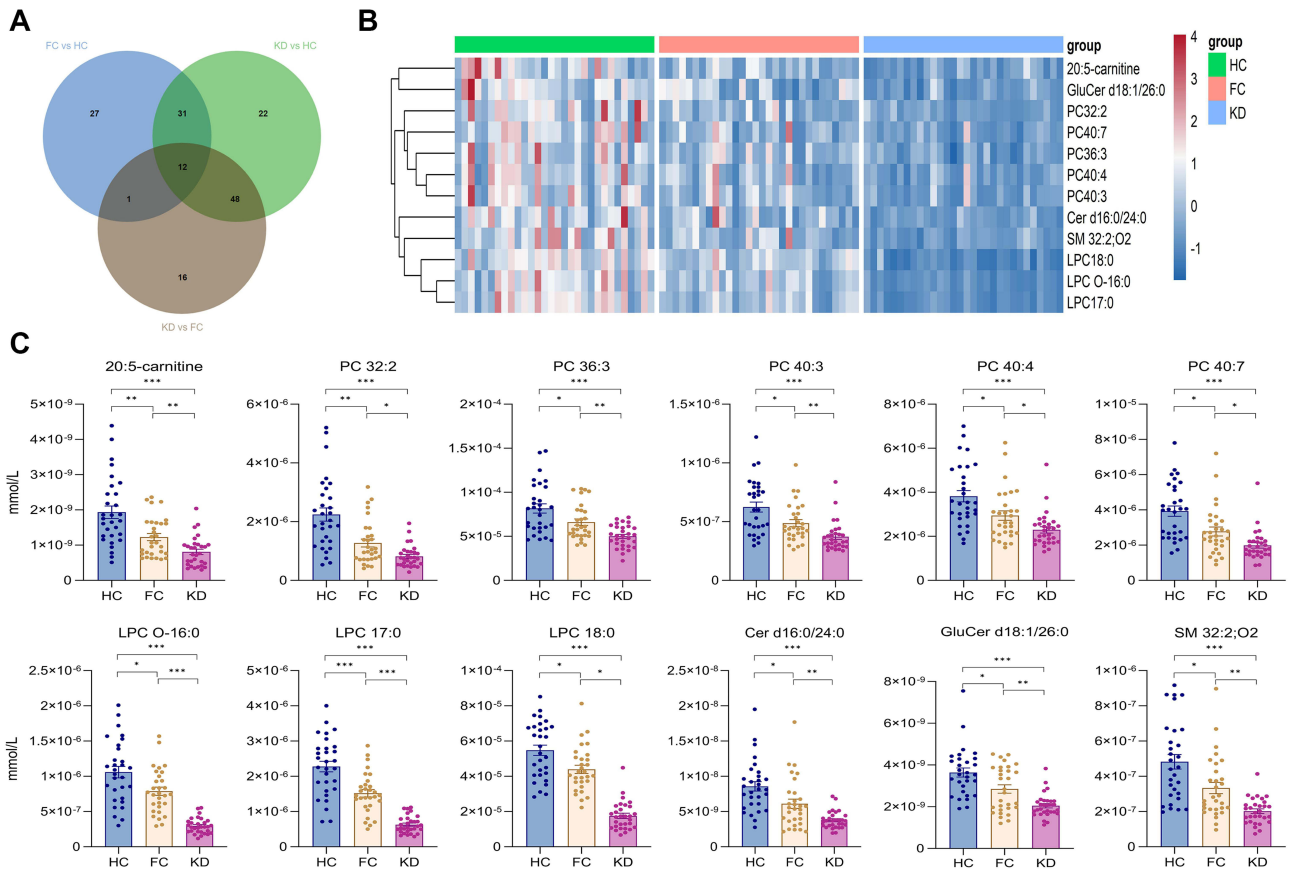

Figure 2 All differential lipid species were downregulated in patients with KD. (**A**) Venn diagram depicting the overlapping significantly altered lipid species identified in the FC vs HC, KD vs HC, and KD vs FC comparisons. (**B**) Clustered heatmap of the three groups across dysregulated lipid species. (**C**) Bar graph showing the expression levels of 12 dysregulated lipid species in the three groups. *$p < 0.05$, **$p < 0.01$, ***$p < 0.001$.
Abbreviations: LPC, lysophosphatidylcholine; Cer, ceramide; SM, sphingomyeli; GluCer, glucosylceramide; PC, phosphatidylcholine.

Screening of Candidate Metabolites

Given the primary objective of identifying early-stage KD biomarkers, we performed an intersection analysis of differential lipid species from pairwise group comparisons, which revealed that 12 metabolites displayed consistent differential alterations (Figure 2A). All data were used for hierarchical clustering in a heatmap to separate the three groups (Figure 2B). In particular, patients with KD displayed lower levels of all identified lipid species — including 20:5-carnitine, SM 32:2;O2, Cer d16:0/24:0, GluCer d18:1/26:0, LPC O-16:0, LPC 17:0, LPC 18:0, PC 32:2, PC 36:3, PC 40:3, PC 40:4, and PC 40:7 — compared with those of the HC and FC groups (Figure 2C).

The random forest algorithm showed that LPC 18:0, LPC 17:0, LPC O-16:0, and Cer d16:0/24:0 were the most significant metabolites in distinguishing patients with KD from both FC (importance scores = 8.2, 6.35, 5.51, and 2.14, respectively) (Figure 3A) and HC (importance scores = 8.4, 5.5, 5.07, and 2.3, respectively) (Figure 3B). A subsequent ROC analysis was performed to clarify their discriminative efficacy. Twelve lipid species showed superior diagnostic performance in distinguishing KD from HC, with area under the curve (AUC) values ranging from 0.841 to 0.987 (Figure S1). Notably, three LPC species—LPC 18:0, LPC 17:0, and LPC O-16:0—consistently achieved AUC values exceeding 0.9, differentiating KD from both HC and FC groups, whereas Cer d16:0/24:0 yielded a slightly lower AUC (0.718) in the KD versus FC comparisons (Figures 3D, S1, and S2).

Next, correlation analyses were performed between the differentially expressed lipids and established clinical inflammatory markers. As shown in Figure 3C, LPC 18:0 demonstrated a significant negative correlation with TNF-α ($r = -0.43$, $P < 0.05$), a key cytokine reflecting disease activity in KD. Likewise, Cer d16:0/24:0 showed a significant inverse correlation with ESR ($r = -0.42$, $P < 0.05$).

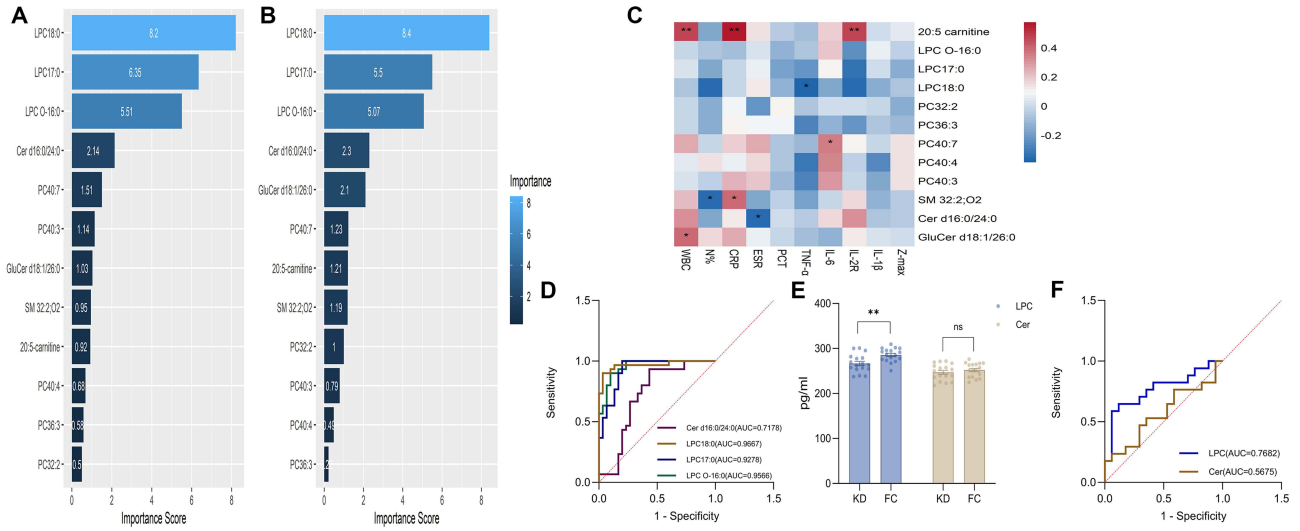

Figure 3 LPC as a potential biomarker for differentiating KD from FC. (**A**) The random forest classifier identifying critical metabolites for distinguishing KD from FC. (**B**) The random forest classifier identifying critical metabolites for distinguishing patients with KD from HC. (**C**) Correlations between the clinical parameters of patients with KD and differentially expressed lipid species. (**D**) ROC curves of the differentially expressed lipid species used to differentiate between KD and FC. (**E**) Bar graph of ELISA-measured LPC and Cer concentrations in the KD and FC groups; *$p < 0.05$, **$p < 0.01$. (**F**) ROC curves for ELISA-measured LPC and Cer concentrations used to distinguish KD from the FC group.

Abbreviations: LPC, lysophosphatidylcholine; Cer, ceramide; SM, sphingomyeli; GluCer, glucosylceramide; PC, phosphatidylcholine.

Validation of Potential Lipid Biomarkers

Therefore, serum levels of LPC and Cer were quantified via ELISA in another validation set. The results showed that patients with KD had significantly lower LPC levels than those of FC ($P < 0.05$), which was consistent with the LC-MS/MS findings (Figure 3E). In addition, the AUC of LPC was 0.768, with 64.7% sensitivity and 88.2% specificity at the optimal threshold (270.56 pg/mL) (Figure 3F). Although Cer levels were lower in the KD group than in the FC group, the difference was not statistically significant ($P > 0.05$). By contrast, there were elevated Cer concentrations in KD compared with those in HC ($P < 0.01$), whereas LPC showed only a non-significant upward trend ($P > 0.05$, Figure S3).

Single-Cell Mapping Reveals Lipid Metabolic Dysregulation

We performed scRNA-seq analysis on PBMCs collected from the participants. After quality control, a total of 109,532 cells were obtained, including 44,728 from the KD group, 42,444 from HC, and 22,360 from FC, which were subsequently clustered into nine major cell types: B cells, CD4+ T cells, CD8+ T cells, dendritic cells, megakaryocytes, monocytes, natural killer (NK) cells, plasma B cells, and γδ T cells (Figure 4A). Immunophenotypic profiling revealed a unique cellular distribution pattern in patients with KD compared with that in controls, characterized by elevated trends in B cells and monocytes, along with declining frequencies of CD8+ T cells and NK cells (Figure 4B).

Based on the 12 significantly decreased lipid species spanning six lipid classes identified in the serum of patients with KD, we retrieved the associated metabolic genes from the published literature and evaluated their expression patterns across the three study groups. In general, genes involved in the synthesis and degradation of Cer, SM, PC, GluCer, carnitine, and LPC were upregulated in the KD group, along with enhanced expression of inflammatory genes (Figure 4C and S4). Consistent with our expectations, a comparative analysis revealed higher inflammatory and lipid metabolism scores in the KD group (Figure 4D and E), particularly in monocytes (Figure 4F and G). Despite showing the highest lipid metabolism score, the low peripheral abundance of dendritic cells and lack of significant differences between the KD and FC groups indicated a minimal contribution to disease-related lipid metabolic perturbations (Figure 4G).

Degradation of LPC is Associated with Monocyte-Mediated Inflammation

We observed that the monocytes of patients with KD had increased expression of lipid metabolism genes, especially compared with those with FC (Figure 5A). Subsequently, Gene Ontology enrichment analysis was performed, which

https://doi.org/10.2147/JIR.S567612

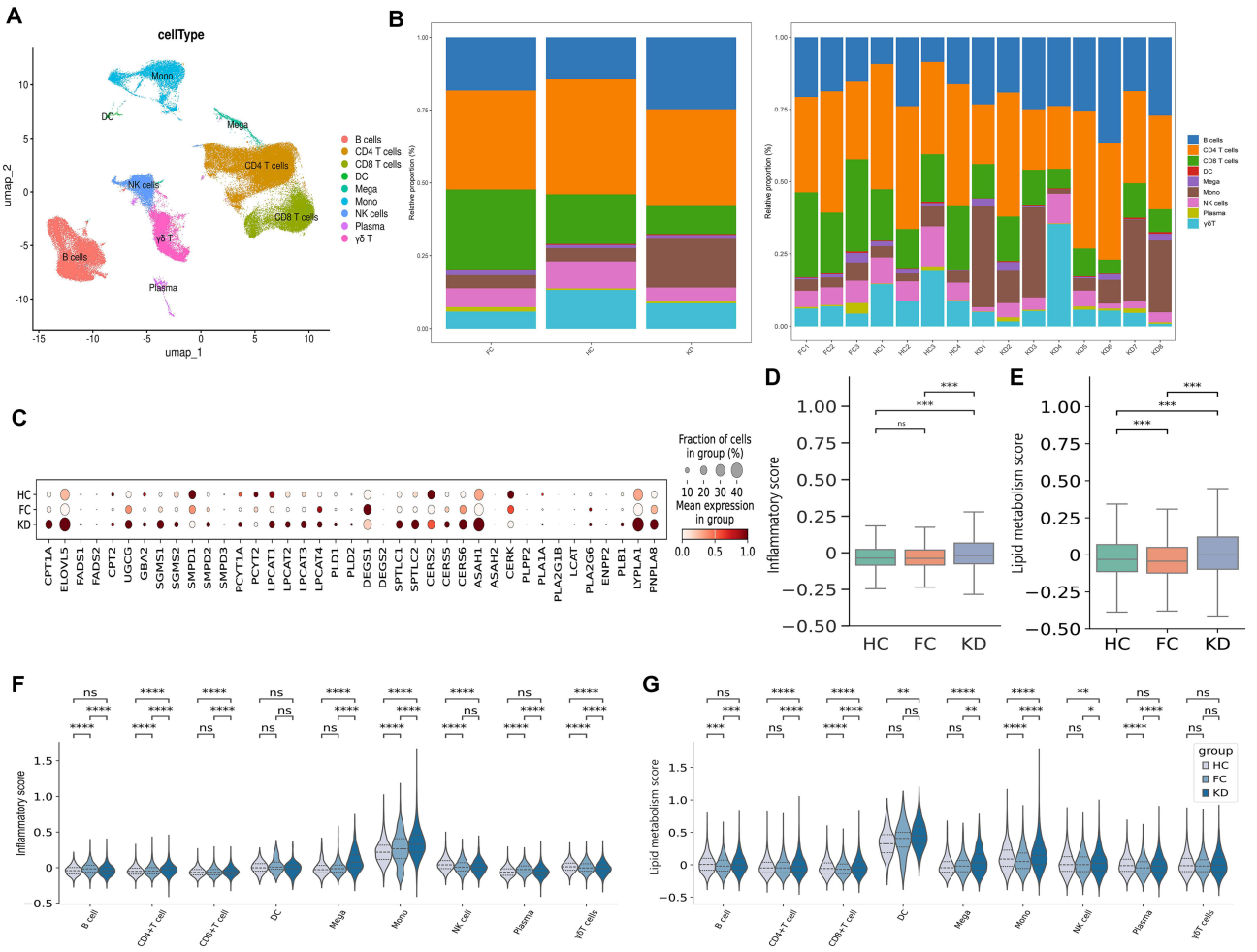

Figure 4 Single-cell RNA sequencing analysis of peripheral blood mononuclear cells harvested from three groups. (**A**) Primary clustering reveals nine major cell types in the integrated single-cell RNA sequencing dataset. (**B**) Proportions of cell clusters across groups and individuals. (**C**) Dot plot of lipid-related metabolic gene expression across the three groups. (**D** and **E**) Box plots of inflammation (left) and lipid metabolism (right) scores across the three groups. (**F** and **G**) Violin plots of inflammatory scores (left) and lipid metabolism scores (right) for the three major cell types. *p < 0.05, **p < 0.01, ***p < 0.001, ****p < 0.0001.

showed that monocytes were primarily involved in phagocytosis, response to oxidative stress, cellular response to chemical stress, and lipid droplet organization (Figure 5B), implying that KD monocytes may acquire an inflammatory activation and metabolically adapted state. Given our identification of LPC as a potential biomarker to distinguish KD from FC in prior metabolomic studies, we examined the correlations between LPC-metabolizing and inflammatory genes. In contrast to genes encoding enzymes that directly or indirectly promote LPC synthesis, genes associated with LPC clearance and degradation exhibited widespread positive correlations with inflammatory gene expression, indicating a highly activated LPC catabolic pathway in KD monocytes (Figure 5C).

Discussion

In this study, we identified lipid metabolic dysregulation during KD onset, manifested specifically as LPC depletion, which has emerged as a potential diagnostic biomarker for KD. Subsequent scRNA-seq analysis revealed upregulated lipid metabolism genes in KD and further demonstrated broadly coordinated alterations between inflammatory genes and those involved in LPC degradation in monocytes. This study integrated lipidomics and scRNA-seq analyses to provide novel insights into inflammation-associated lipidomic alterations in KD.

Few studies have described changes in the lipid metabolism profiles of KD. However, significant correlations between multiple lipid species and inflammatory markers were observed in our study, indicating their potential involvement in the inflammatory processes in KD. Lipids play a crucial role in maintaining cellular integrity and physiological functions,[18]

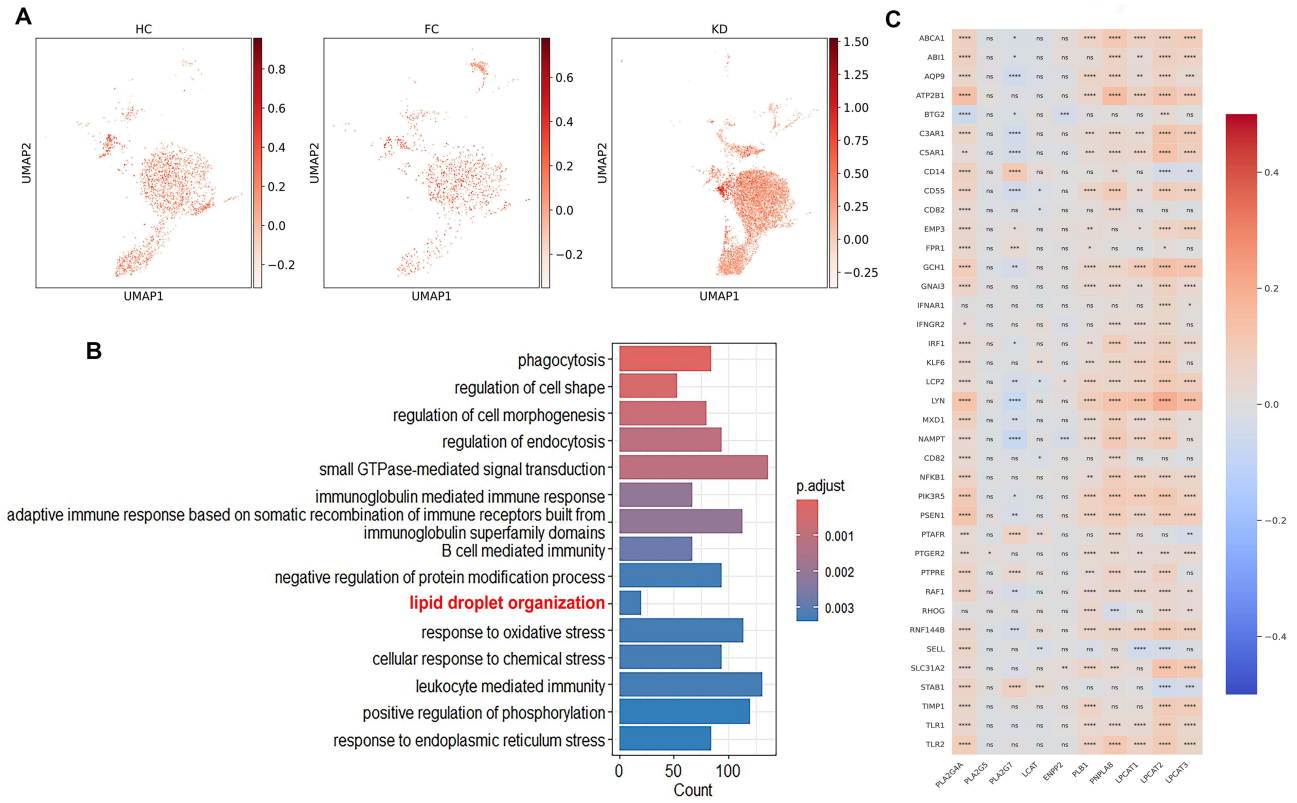

Figure 5 LPC catabolism links monocyte metabolic adaptation to inflammation in KD. (**A**) Uniform Manifold Approximation and Projection (UMAP): lipid metabolism score distribution across monocyte subsets (KD vs FC vs HC). (**B**) Top 15 enriched Gene Ontology pathways of differentially expressed genes in monocytes of patients with KD compared with those with FC. (**C**) Heatmap of the correlation between inflammatory and LPC-related metabolic genes. *$p < 0.05$, **$p < 0.01$, ***$p < 0.001$, ****$p < 0.0001$. **Abbreviation**: LPC, lysophosphatidylcholine.

and thus, any perturbation in lipid metabolism can have profound consequences on cellular and organismal health. Nakashima et al reported that elevated levels of oxidized PC may engage lectin-like oxidized low-density lipoprotein receptor-1-dependent signaling cascades, thereby contributing to the pathogenesis of coronary arteritis in KD.[14] In parallel, genetic evidence has emerged to support a positive causal link between PC and KD.[19] Similar lipid abnormalities appear in many immune disorders. For instance, several increased PC species containing unsaturated fatty acids were good predictors of the presence of coronary calcification in patients with systemic lupus erythematosus.[20] In addition, diverse Cer species exhibit markedly elevated levels in the sera of patients with rheumatoid arthritis across disease activity strata,[21] activating synovial cells and promoting disease progression.[22] These findings suggest that aberrant lipid signaling is a common nexus that bridges metabolic alterations and inflammatory immunity, highlighting its translational potential as a diagnostic biomarker.

LPC, an important component of the lipid metabolic network, was recognized as a promising biomarker for KD in our study, with decreased levels observed in patients with KD. Analogous dysregulation of LPC metabolism occurs in other inflammatory diseases.[23–25] The reasons may include the following. Firstly, LPC clearance is likely enhanced under high inflammatory conditions, though the specific mechanism remains unknown. Our present scRNA-seq analysis illustrated the coordinated expression of inflammatory genes and genes encoding LPC-catabolizing enzymes in monocytes. This suggests that under highly inflammatory conditions, monocytes, which are the major immune effector cells in KD, may upregulate LPC-degrading enzyme expression to accelerate clearance from the circulation and tissue. In parallel, we also observed that the "lipid droplet organization" pathway was significantly enriched in monocytes. In addition to their fundamental role in energy storage, lipid droplets have been demonstrated to influence signal transduction, cellular stress mitigation, membrane biogenesis, and transcriptional regulation.[26] Accumulating evidence has emphasized their high dynamism as organelles, whose formation is modulated in response to environmental stimuli.[27] Accordingly, these

https://doi.org/10.2147/JIR.S567612

adaptive responses led us to propose that monocytes may regulate the lipid microenvironment through metabolic reprogramming, thereby suppressing excessive inflammation and mitigating tissue damage in patients with KD. Secondly, the frequent occurrence of hypoalbuminemia in KD patients[28] could contribute to reduced LPC level. Most plasma LPC resides in the albumin fraction,[29] thus the absence of this primary carrier protein may render free LPC particularly susceptible to accelerated clearance. Thirdly, platelet activation in KD provides an additional possible explanation. As a common pathological feature in KD,[30] its activation may release autotaxin (ATX), which catalyzes LPC conversion to lysophosphatidic acid (LPA),[31] thereby reducing circulating LPC level.

LPC is an important lipid molecule that regulates inflammatory responses, whereas its involvement in the pathological process of KD remains unclear. Fundamental evidence has demonstrated LPC's potent ability to induce the formation of neutrophil extracellular traps (NETs) by promoting the burst of reactive oxygen species (ROS) through various pathways.[32,33] Meanwhile, the conversion of LPC to the more bioactive LPA can further amplify the signaling for NETs formation. Notably, previous studies have reported excessively released NETs contribute to inflammatory progression in KD[34] and are implicated in driving the development of CAL.[35] Based on current research and existing literature, we hypothesize that LPC may function as an "inflammatory trigger" to initiate the inflammatory cascade in the disease onset. However, during the progression of the disease, LPC might be extensively depleted, converted, and cleared driven by metabolic reprogramming under the hyperinflammatory state, resulting in decreased LPC level in plasma. Chen et al reported that the alleviation of inflammation following IVIG treatment was accompanied by elevated LPC level,[11] further supporting the negative correlation between LPC and high inflammatory status in the early disease stage before IVIG treatment. In addition to the aforementioned, LPC may also be implicated in other mechanisms underlying the pathological process of KD. Liang et al found that LPC can indirectly enhance the post-translational modification of the NOD-like receptor family pyrin domain-containing 3 (NLRP3) and promote its pathological activation through a murine experiment.[36] Importantly, recent studies on KD have highlighted IL-1β signaling as central to pathogenesis,[37] with NLRP3 inflammasome activation being essential for IL-1β maturation and release.[38]

Interestingly, specific LPC species with different chain lengths and saturation may exert distinct biological functions. For example, LPC 20:4 and LPC 22:6 have been shown to possess anti-inflammatory effects in a murine model.[39] Zhen et al also revealed a negative causal relationship between LPC (0:0/20:0) and KD risk using a Mendelian randomization analysis.[19] In light of our observation that genes encoding LPC-catabolizing enzymes were broadly upregulated in association with inflammation, it is thus plausible that such protective LPC species may likewise be non-selectively cleared, which could exacerbate systemic inflammation. Taken together, LPC appears to be a dynamically changing key mediator in the pathophysiological processes of KD, yet the direct mechanisms remain to be fully elucidated.

A key challenge in the clinical diagnosis of KD is its differentiation from febrile diseases. Therefore, in the design of the control group for this study, we not only included healthy children but also selected age- and sex-matched children with infectious fever. Compared with HC, patients with KD exhibited a more pronounced reduction in differential lipid levels than those with FC, despite similar metabolic changes, suggesting more severe and specific metabolic disturbances in KD, likely attributable to distinct immunopathological mechanisms. The pathogenesis of KD is currently considered a dysregulated immune response triggered by exposure to specific pathogens in genetically predisposed individuals,[40] and although the same infectious state exists, different pathogens may induce different immunometabolic responses in the host.[41,42] Furthermore, abnormal immune activation and persistent inflammation may lead to increased lipid consumption, impaired synthesis, or redirected lipid metabolic pathways that accommodate cellular activities.[43,44] Given these distinctions, novel application prospects have arisen for the development of diagnostic strategies to distinguish between KD and FC from a metabolic perspective.

This study had several limitations. First, this study was conducted at a single center with a limited sample size, particularly in the validation set, and with only internal validation performed, which may affect the general applicability of the identified biomarkers. Larger-scale, multi-center prospective cohort studies are needed to clarify the diagnostic value. Second, our study did not include patients with incomplete KD, which may limit the generalizability of our findings to the full spectrum of KD presentations. Third, this study only collected samples at a single time point before treatment, thus failing to reveal the dynamic change patterns of LPC during disease progression. Given the complex role LPC may play in the pathological mechanism of KD, it is necessary to conduct dynamic monitoring of LPC in future

studies. Finally, our study only suggested metabolic and transcriptomic changes, and the in-depth mechanisms underlying the interaction between immunity and lipid metabolism require further exploration.

Conclusion

Collectively, our study integrated serum metabolomic and scRNA-seq data to characterize inflammation-driven lipid metabolic dysregulation in KD and identify potential LPC biomarkers. We believe that these findings not only contribute to early diagnosis in clinical practice but also yield valuable insights into the pathophysiological mechanisms underlying KD.

Abbreviations

Cer, ceramide; CAL, coronary artery lesions; FC, febrile controls; GluCer, glucosylceramide; HC, healthy controls; IL, interleukin; KD, Kawasaki disease; LPC, lysophosphatidylcholine; LC-MS/MS, liquid chromatography-tandem mass spectrometry; PC, phosphatidylcholine; scRNA-seq, single-cell RNA sequencing; SM, sphingomyelin; TNF, tumor necrosis factor; UMAP, uniform manifold approximation and projection.

Data Sharing Statement

All omics data have been deposited in the China National Center for Bioinformation (OMIX013207, OMIX013211 and OMIX013239).

Ethics Approval and Informed Consent

This study was approved by the Ethics Committee of the Capital Institute of Pediatrics (SHERLL2022006). Informed consent was obtained from all parents or legal guardians of the participants and for publishing potentially identifiable medical information.

Author Contributions

Xiaomei Ma: conceptualization, formal analysis, methodology, visualization, writing – original draft, writing – review & editing, software; Yang Zheng: conceptualization, investigation, data curation, writing – original draft, supervision; Chenhui Feng: formal analysis, visualization, software, methodology, writing – review & editing; Mingming Zhang: investigation, data curation, supervision, visualization, writing – review & editing; Hongmao Wang: supervision, project administration, visualization, data curation, investigation, writing – review & editing;

Xiaohui Li: conceptualization, supervision, resources, funding acquisition, writing – review & editing, investigation.

All authors gave final approval of the version to be published; have agreed on the journal to which the article has been submitted; and agree to be accountable for all aspects of the work.

Funding

This work was supported by the National Natural Science Foundation of China (82370511) and the Beijing Research Ward Excellence Program (BRWEP2024W102100107).

Disclosure

The authors report no conflicts of interest in this work.

References

1. Fukazawa R, Kobayashi J, Ayusawa M, et al. JCS/JSCS 2020 guideline on diagnosis and management of cardiovascular sequelae in Kawasaki disease. *Circ J*. 2020;84(8):1348–1407. doi:10.1253/circj.CJ-19-1094
2. McCrindle BW, Rowley AH, Newburger JW, et al. Diagnosis, treatment, and long-term management of Kawasaki disease: a scientific statement for health professionals from the American heart association. *Circulation*. 2017;135(17):e927–e999. doi:10.1161/CIR.0000000000000484
3. Zhang R, Shuai S, Zhang H, et al. Predictive value of albumin for intravenous immunoglobulin resistance in a large cohort of Kawasaki disease patients. *Ital J Pediatr*. 2023;49(1):78. doi:10.1186/s13052-023-01482-z

4. Ganguly M, Nandi A, Banerjee P, et al. A comparative study of IL-6, CRP and NT-proBNP levels in post-COVID multisystem inflammatory syndrome in children (MISC) and Kawasaki disease patients. *Int J Rheum Dis*. 2022;25(1):27–31. doi:10.1111/1756-185X.14236
5. Xiu-Yu S, Jia-Yu H, Qiang H, et al. Platelet count and erythrocyte sedimentation rate are good predictors of Kawasaki disease: ROC analysis. *J Clin Lab Anal*. 2010;24(6):385–388. doi:10.1002/jcla.20414
6. Pattanaik SS, Panda AK, Pati A, et al. Role of interleukin-6 and interferon-α in systemic lupus erythematosus: a case-control study and meta-analysis. *Lupus*. 2022;31(9):1094–1103. doi:10.1177/09612033221102575
7. Zhai GH, Zhang W, Xiang Z, et al. Diagnostic value of sIL-2R, TNF-α and PCT for sepsis infection in patients with closed abdominal injury complicated with severe multiple abdominal injuries. *Front Immunol*. 2021;12:741268. doi:10.3389/fimmu.2021.741268
8. Lin Z, Long F, Yang Y, et al. Serum ferritin as an independent risk factor for severity in COVID-19 patients. *J Infect*. 2020;81(4):647–679. doi:10.1016/j.jinf.2020.06.053
9. Graça ICR, Martins C, Ribeiro F, et al. Understanding hypertension: a metabolomic perspective. *Biology*. 2025;14(4):403. doi:10.3390/biology14040403
10. Zhao Y, Ma C, Cai R, et al. NMR and MS reveal characteristic metabolome atlas and optimize esophageal squamous cell carcinoma early detection. *Nat Commun*. 2024;15(1):2463. doi:10.1038/s41467-024-46837-0
11. Chen Z, Sai S, Nagumo K, et al. Distinctive serum lipidomic profile of IVIG-resistant Kawasaki disease children before and after treatment. *PLoS One*. 2023;18(3):e0283710. doi:10.1371/journal.pone.0283710
12. Wang X, Han L, Jiang J, et al. Alterations in bile acid metabolites associated with pathogenicity and IVIG resistance in Kawasaki disease. *Front Cardiovasc Med*. 2025;12:1549900. doi:10.3389/fcvm.2025.1549900
13. Zhu Q, Dong Q, Wang X, et al. Palmitic acid, A critical metabolite, aggravates cellular senescence through reactive oxygen species generation in Kawasaki disease. *Front Pharmacol*. 2022;13:809157. doi:10.3389/fphar.2022.809157
14. Nakashima Y, Sakai Y, Mizuno Y, et al. Lipidomics links oxidized phosphatidylcholines and coronary arteritis in Kawasaki disease. *Cardiovasc Res*. 2021;117(1):96–108. doi:10.1093/cvr/cvz305
15. Chen Y, Yang M, Zhang M, et al. Single-cell transcriptome reveals potential mechanisms for coronary artery lesions in Kawasaki disease. *Arterioscler Thromb Vasc Biol*. 2024;44(4):866–882. doi:10.1161/ATVBAHA.123.320188
16. O'Neill LA, Kishton RJ, Rathmell J. A guide to immunometabolism for immunologists. *Nat Rev Immunol*. 2016;16(9):553–565. doi:10.1038/nri.2016.70
17. Kobayashi T, Fuse S, Sakamoto N, et al. A new Z score curve of the coronary arterial internal diameter using the lambda-mu-sigma method in a pediatric population. *J Am Soc Echocardiogr*. 2016;29(8):794–801.e729. doi:10.1016/j.echo.2016.03.017
18. Yoon H, Shaw JL, Haigis MC, et al. Lipid metabolism in sickness and in health: emerging regulators of lipotoxicity. *Mol Cell*. 2021;81(18):3708–3730. doi:10.1016/j.molcel.2021.08.027
19. Zhen C, Zhang S, Guo F. Specific plasma lipid species in children are causally associated with kawasaki disease: a mendelian randomization analysis. *Ital J Pediatr*. 2025;51(1):285. doi:10.1186/s13052-025-02126-0
20. Urbain F, Ponnaiah M, Ichou F, et al. Impaired metabolism predicts coronary artery calcification in women with systemic lupus erythematosus. *EBioMedicine*. 2023;96:104802. doi:10.1016/j.ebiom.2023.104802
21. Migita K, Honda S, Yamasaki S, et al. Regulation of rheumatoid synovial cell growth by ceramide. *Biochem Biophys Res Commun*. 2000;269(1):70–75. doi:10.1006/bbrc.2000.2239
22. Luan H, Chen S, Zhao L, et al. Precise lipidomics decipher circulating ceramide and sphingomyelin cycle associated with the progression of rheumatoid arthritis. *J Proteome Res*. 2023;22(12):3893–3900. doi:10.1021/acs.jproteome.3c00574
23. Li R, Koh JH, Park WJ, et al. Serum and urine lipidomic profiles identify biomarkers diagnostic for seropositive and seronegative rheumatoid arthritis. *Front Immunol*. 2024;15:1410365. doi:10.3389/fimmu.2024.1410365
24. Urbanski G, Chabrun F, Delattre E, et al. An immuno-lipidomic signature revealed by metabolomic and machine-learning approaches in labial salivary gland to diagnose primary Sjögren's syndrome. *Front Immunol*. 2023;14:1205616. doi:10.3389/fimmu.2023.1205616
25. Zhang Q, Li X, Yin X, et al. Metabolomic profiling reveals serum L-pyroglutamic acid as a potential diagnostic biomarker for systemic lupus erythematosus. *Rheumatology*. 2021;60(2):598–606. doi:10.1093/rheumatology/keaa126
26. Zadoorian A, Du X, Yang H. Lipid droplet biogenesis and functions in health and disease. *Nat Rev Endocrinol*. 2023;19(8):443–459. doi:10.1038/s41574-023-00845-0
27. Prevost CT, Gansereit WB, Kashatus DF. NRF2 regulates lipid droplet dynamics to prevent lipotoxicity. *Iscience*. 2025;28(7):112925. doi:10.1016/j.isci.2025.112925
28. Mammadov G, Liu HH, Chen WX, et al. Hepatic dysfunction secondary to Kawasaki disease: characteristics, etiology and predictive role in coronary artery abnormalities. *Clin Exp Med*. 2020;20(1):21–30. doi:10.1007/s10238-019-00596-1
29. Tan ST, Ramesh T, Toh XR, et al. Emerging roles of lysophospholipids in health and disease. *Prog Lipid Res*. 2020;80:101068. doi:10.1016/j.plipres.2020.101068
30. Zhang Y, Wang Y, Zhang L, et al. Reduced platelet miR-223 induction in Kawasaki disease leads to severe coronary artery pathology through a miR-223/PDGFRβ vascular smooth muscle cell axis. *Circ Res*. 2020;127(7):855–873. doi:10.1161/CIRCRESAHA.120.316951
31. Smyth SS, Kraemer M, Yang L, et al. Roles for lysophosphatidic acid signaling in vascular development and disease. *Biochim Biophys Acta Mol Cell Biol Lipids*. 2020;1865(8):158734. doi:10.1016/j.bbalip.2020.158734
32. Awasthi D, Nagarkoti S, Kumar A, et al. Oxidized LDL induced extracellular trap formation in human neutrophils via TLR-PKC-IRAK-MAPK and NADPH-oxidase activation. *Free Radic Biol Med*. 2016;93:190–203. doi:10.1016/j.freeradbiomed.2016.01.004
33. Liu S, Wang Y, Ying L, et al. Quercetin mitigates lysophosphatidylcholine (LPC)-induced neutrophil extracellular traps (NETs) formation through inhibiting the P2X7R/P38MAPK/NOX2 pathway. *Int J Mol Sci*. 2024;25(17):9411.
34. Jin J, Zhao Y, Fang Y, et al. Neutrophil extracellular traps promote the activation of the NLRP3 inflammasome and PBMCs pyroptosis via the ROS-dependent signaling pathway in Kawasaki disease. *Int Immunopharmacol*. 2025;145:113783. doi:10.1016/j.intimp.2024.113783
35. Hamamichi Y, Ichida F, Yu X, et al. Neutrophils and mononuclear cells express vascular endothelial growth factor in acute Kawasaki disease: its possible role in progression of coronary artery lesions. *Pediatr Res*. 2001;49(1):74–80. doi:10.1203/00006450-200101000-00017
36. Liang S, Zhou J, Cao C, et al. GITR exacerbates lysophosphatidylcholine-induced macrophage pyroptosis in sepsis via posttranslational regulation of NLRP3. *Cell Mol Immunol*. 2024;21(7):674–688. doi:10.1038/s41423-024-01170-w

37. Koné-Paut I, Tellier S, Belot A, et al. Phase II open label study of anakinra in intravenous immunoglobulin-resistant Kawasaki disease. *Arthritis Rheumatol*. 2021;73(1):151–161. doi:10.1002/art.41481
38. Atici AE, Noval Rivas M, Arditi M. The central role of interleukin-1 signalling in the pathogenesis of kawasaki disease vasculitis: path to translation. *Can J Cardiol*. 2024;40(12):2305–2320. doi:10.1016/j.cjca.2024.07.023
39. Hung ND, Sok DE, Kim MR. Prevention of 1-palmitoyl lysophosphatidylcholine-induced inflammation by polyunsaturated acyl lysophosphatidylcholine. *Inflamm Res*. 2012;61(5):473–483. doi:10.1007/s00011-012-0434-x
40. Wang W, Zhu L, Li X, et al. Emerging evidence of microbial infection in causing systematic immune vasculitis in Kawasaki disease. *Front Microbiol*. 2023;14:1313838. doi:10.3389/fmicb.2023.1313838
41. Wegermann K, Lucas JE, Dubois L, et al. Plasma lipid metabolites differentiate metabolic from viral chronic liver disease. *J Infect Dis*. 2025;232 (2):346–358. doi:10.1093/infdis/jiaf270
42. Xia W, Mao Y, Xia Z, et al. Metabolic remodelling produces fumarate via the aspartate-argininosuccinate shunt in macrophages as an antiviral defence. *Nat Microbiol*. 2025;10(5):1115–1129. doi:10.1038/s41564-025-01985-x
43. Prevete N, Liotti F, Amoresano A, et al. New perspectives in cancer: modulation of lipid metabolism and inflammation resolution. *Pharmacol Res*. 2018;128:80–87. doi:10.1016/j.phrs.2017.09.024
44. Zhang C, Wang K, Yang L, et al. Lipid metabolism in inflammation-related diseases. *Analyst*. 2018;143(19):4526–4536. doi:10.1039/C8AN01046C